5-15-2009

X-Ray Magnetic Circular Dichroism of Pulsed Laser Deposited Co2MnSn and Co2MnSb Thin Films Grown on GaAs (001)

Moti R. Paudel
Southern Illinois University Carbondale

Christopher S. Wolfe
Southern Illinois University Carbondale

Naushad Ali
Southern Illinois University Carbondale

Shane Stadler
Southern Illinois University Carbondale

Joseph A. Christodoulides
Naval Research Laboratory

See next page for additional authors

Published in *Journal of Applied Physics*, Vol. 105 No. 10 (2009) at doi: 10.1063/1.3126502

X-ray magnetic circular dichroism of pulsed laser deposited Co_2MnSn and Co_2MnSb thin films grown on GaAs (001)

Moti R. Paudel,[1,a)] Christopher S. Wolfe,[1] Naushad Ali,[1] Shane Stadler,[1,b)] Joseph A. Christodoulides,[2] David L. Ederer,[3] Yinwan Li,[3] Thomas A. Callcott,[4] and John W. Freeland[5]

[1]*Department of Physics, Southern Illinois University, Neckers 483 A, Carbondale, Illinois 62901, USA*
[2]*Naval Research Laboratory, Code 6360, 4555 Overlook Avenue SW, Washington, DC 20375-5320, USA*
[3]*Department of Physics, Tulane University, 2001 Percival Stern Hall, New Orleans, Louisiana 70118, USA*
[4]*Department of Physics, University of Tennessee at Knoxville, 611 Science and Engineering Building, 1414 Circle Drive, Knoxville, Tennessee 37996-1200, USA*
[5]*Advanced Photon Source, Argonne National Laboratory, 9700 S. Cass Ave, Argonne, Illinois 60439, USA*

(Received 30 October 2008; accepted 3 April 2009; published online 22 May 2009)

We present the structural and element specific magnetic properties of Co_2MnSn and Co_2MnSb thin films grown on GaAs (100) substrates using pulsed laser deposition. X-ray magnetic circular dichroism (XMCD) spectra were measured for 400 Å thick films at the $L_{2,3}$ edges of Co and Mn. Element specific moments for Co and Mn in Co_2MnSn were calculated from the x-ray absorption and XMCD spectra using the XMCD sum rules. The ratios of orbital to spin magnetic moments for Co and Mn were calculated for Co_2MnSn and Co_2MnSb. © *2009 American Institute of Physics*. [DOI: 10.1063/1.3126502]

INTRODUCTION

Half-metallic ferromagnets have only one spin channel for conduction at the Fermi level, where the other channel has a band gap across the Fermi level. There is a particular interest in the use of these alloys in electronic devices that exploit both the spin and the charge of the electron, including spin injection devices, giant magnetoresistant materials, and nonvolatile magnetic random access memory elements that operate ideally at or above room temperature.[1–3]

The search for half-metallic materials has a long history that starts from de Groot *et al.*, when they predicted the first half-metallic compound, NiMnSb, through band structure calculations.[4] Since then, several other compounds have been predicted to be half-metallic including other half-Heuslers such as PtMnSb;[5,6] full-Heusler alloys such as Co_2MnSi and Co_2MnGe;[7,8] metallic ferromagnetic oxides such as CrO_2;[9] manganites such as $La_{0.7}Sr_{0.3}MnO_3$;[9–11] double perovskites such as Sr_2FeReO_6;[12] the pnictides such as CrAs in the zinc-blende structure;[13] pyrites such as CoS_2;[14] transition metal chalcogenides such as CrSe;[15] and dilute magnetic semiconductors such as Mn-doped Si and GaAs.[16,17]

The practical realization of these half-metallic materials resides in the field of spintronics and requires a thin film form of the half-metallic compounds on semiconductor and other types of substrates. High Curie temperatures and magnetic moments, as well as large minority band gaps, are desired for practical applications. In particular, one needs to prevent the reduction in magnetic properties by thermal effects in room temperature devices. Several experiments have been done so far on the abovementioned half-metallic materials, however, none of them have been found to be perfectly half-metallic at room temperature. Many predicted half-metals exhibit a dramatic decrease in spin polarization and junction magnetoresistance well below room temperature. Experimentally, some of these materials, such as CrO_2 and $La_{0.7}Sr_{0.3}MnO_3$, were found to have almost 100% spin polarization at a temperature near 1 K.[10,11] They have fairly low Curie temperatures and possess an undesirable critical nature (magnetically disordered termination layer) of the interface between these oxides and the material into which spins are to be injected. Moreover CrO_2 is difficult to fabricate since the structure is metastable. These things limit the potential practical realization of these materials in devices. Since some of the practical goals include spin injection into semiconductors and use in tunneling phenomena at layered interfaces, we need to explore the thin film properties deposited on semiconducting substrates. Moreover, one of the main issues is that of the surface stability of the polarization.[18]

Full Heusler alloys (X_2YZ) that crystallize in the $L2_1$ structure are composed of four interpenetrating fcc sublattices. Many of them have high Curie temperatures, large magnetic moments, and large (predicted) minority gaps in the spin density of states, all of which are desirable properties for spintronics applications. However, due to the presence of antisite disorder, in addition to many other possible defects in real materials, there is the appearance of minority spin states at the Fermi level, which effectively destroys the predicted spin polarization.[8,9] Following the band structure calculations of Ishida *et al.*, Co_2MnSb and Co_2MnSn are not 100% spin polarized, but their mixed alloys, $Co_2MnSn_xSb_{1-x}$ for the range of $0.2<x<0.6$, are predicted to be half-metallic.[7] To the best of our knowledge, this series of

[a)]Author to whom correspondence should be addressed. Electronic mail: motirajpaudel@yahoo.com. Presently at the Department of Oncology, Cross Cancer Institute, University of Alberta, Edmonton, Alberta, Canada T6G 1Z2.
[b)]Presently at the Department of Physics and Astronomy, Louisiana State University, Baton Rouge, Louisiana 70802.

compounds has found little attention in the experimental literature until recently. In this paper we present the structural and element specific magnetic properties of thin films of Co_2MnSn and Co_2MnSb grown on GaAs (100) substrates fabricated using pulsed laser deposition techniques. The mixed alloys with $0.2<x<0.6$ will be addressed in a future study.

EXPERIMENT

Polycrystalline bulk buttons of $Co_2MnSn_xSb_{1-x}$ ($x=0$ and 1) alloys (approximately 5 g) were fabricated using conventional arc melting procedures in an argon atmosphere using commercially available elements with 4*N* purity. The elements were melted three times and the weight loss after melting was found to be less than 0.2%. To enhance the homogeneity, they were wrapped in tantalum foil and annealed in vacuum ($<10^{-4}$ Torr) at 850 °C for 24 h. For the growth of film samples, thick disks of the bulk alloys thus prepared were mirror polished using sand paper in ethyl alcohol to avoid oxidation and were used as targets. The films were grown on American flat GaAs (100). The substrates were first ramped to 600 °C, and then held at that temperature for 15 min inside an ultrahigh vacuum chamber in order to remove oxides present on the surface and to reconstruct the surface.[19] The substrate was then slowly cooled down to 178 °C for deposition. Prior to film deposition, the targets were conditioned with the laser in order to remove any oxides formed on the surface.

Thin films were grown in an ultrahigh vacuum pulsed laser deposition chamber with a base pressure less than 1×10^{-8} Torr. The deposition source was a KrF ($\lambda=248$ nm) excimer laser with a 20 ns pulse duration and a 10 Hz repetition rate. The target to substrate distance was about 42 mm and the laser fluence was around 4 J/cm^2. The deposition rates were monitored with a quartz crystal monitor and were calibrated using Rutherford backscattering (RBS). RBS was also used to monitor the stoichiometry of both the targets and the film samples. We have concentrated on the samples grown with overall deposition rates around 20 Å/min and having a thickness of 400 Å with an error of ±5%.

Structural phases were identified through x-ray diffraction (XRD) measurements at room temperature using a GBC MMA x-ray diffractometer in Bragg–Brentano geometry using Cu $K\alpha$ radiation. The XRD scans were indexed using POWDERCELL™ commercial software.[20] The compositional analysis was done with RBS and was further confirmed using x-ray fluorescence (XRF) spectroscopic measurements. The element specific magnetic information was obtained using x-ray magnetic circular dichroism (XMCD) measured at beamline 4-ID-C of the Advanced Photon Source at Argonne National Laboratory.

RESULTS AND DISCUSSION

Room temperature XRD patterns of typical Co_2MnSn and Co_2MnSb (400 Å) thin films are shown in Fig. 1. Due to the highly oriented nature of the GaAs (100) substrates, in addition to the film peaks we observed Cu $K\beta$ peaks, and also W $K\alpha$ contamination peaks due to the x-ray emission from the tungsten filament in the Cu x-ray tube. The Co_2MnSn film was primarily (220) orientated, whereas the Co_2MnSb film, constructed under similar growth conditions and of the same thickness, shows a (100)-orientation. In Fig. 1(b), the peak labeled as GaAs (220) results from the slight miscut of the substrate from the (100) plane (usually around 0.2°). This feature is barely discernable in Fig. 1(a), but is present under close inspection, as it is on blank substrates. The positions of the film peaks were shifted slightly from their bulk positions, which could partially be due to the strain of the GaAs substrate resulting from lattice mismatch (~5%). The lattice constants of the Co_2MnSn and Co_2MnSb thin films were estimated to be $a=5.78$ and 5.98 Å, compared to their bulk values of $a=6.00$ and 5.94 Å, respectively. The reason why the Co_2MnSn film is compressed and the Co_2MnSb film remains nearly unstrained relative to the bulk is not known and requires a detailed structural study. An extra peak was also observed in all of the scans [indicated by an asterisk (*)], which was confirmed to be from the Al-alloy sample holder. Although we made $Co_2MnSn_xSb_{1-x}$ films of three concentrations ($x=0$, 0.5, and 1), due to the oxidation of the $x=0.5$ samples, we only have characterized the films using XMCD for $x=0$ and 1.

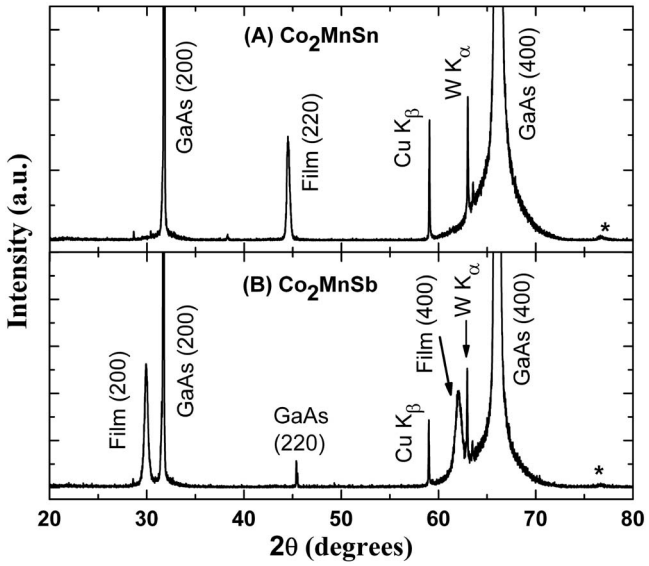

FIG. 1. Room temperature XRD patterns of (a) Co_2MnSn(400 Å)/GaAs (100) and (b) Co_2MnSb(400 Å)/GaAs (100). The asterisks (*) indicate the sample holder peaks (Al alloy).

The RBS and XRF measurements for the composition analysis show that both of the films are *sp* element (Sb and Sn) deficient and Mn rich. In the case of the Co_2MnSb film, the RBS measurement showed the composition to be $Co_{2.04}Mn_{1.28}Sb_{0.68}$, whereas the XRF result showed $Co_{2.20}Mn_{1.30}Sb_{0.50}$. Since our targets were confirmed to be of correct composition using inductively coupled plasma spectroscopy, the noncongruent transfer to the substrates must be addressed. The failure to transfer the correct composition from the target to the film could be due to nonoptimal deposition conditions such as insufficient fluence or geometric factors such as target to substrate distance. More likely, preferential ablation may occur at grain boundaries, thereby de-

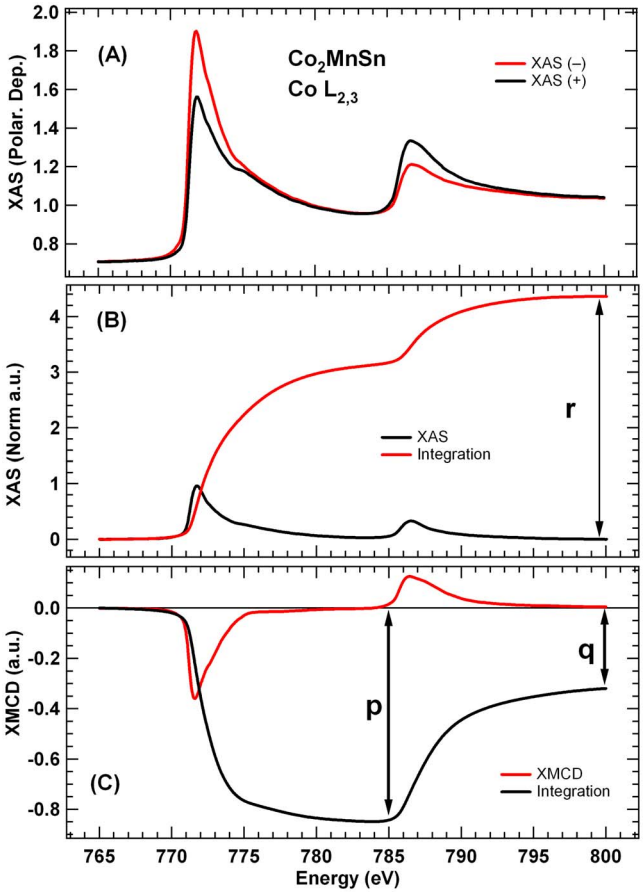

FIG. 2. (Color online) Polarization-dependent Co $L_{2,3}$ XAS and XMCD spectra for Co_2MnSn(400 Å)/GaAs (100) capped with 40 Å Al.

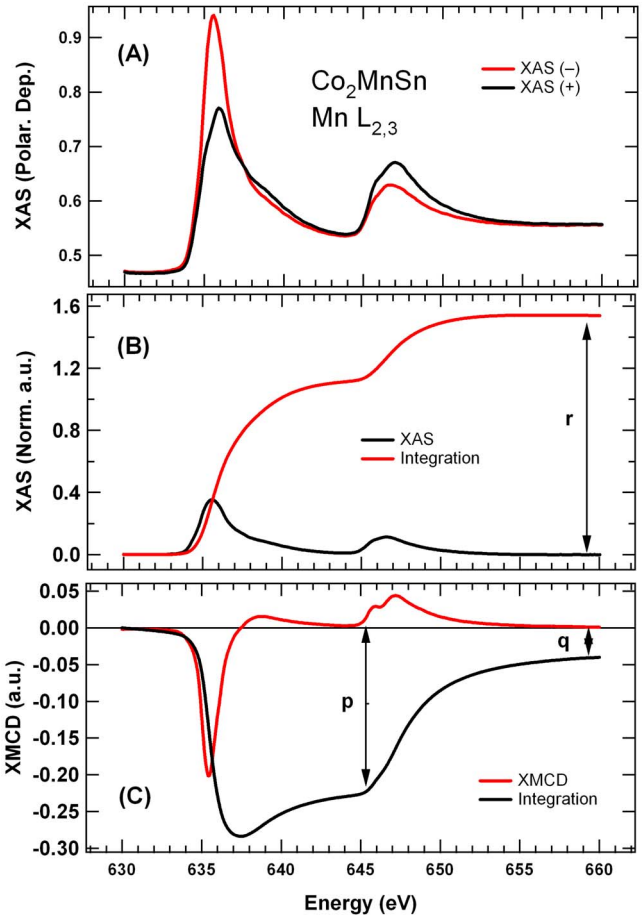

FIG. 3. (Color online) Polarization-dependent Mn $L_{2,3}$ XAS and XMCD spectra for Co_2MnSn(400 Å)/GaAs (100) capped with 40 Å Al.

pleting any constituent that may migrate to the boundary. This occurrence could possibly be alleviated by using single crystal targets.

The XMCD measurements were carried out on 400 Å thick Co_2MnSn and Co_2MnSb films grown on GaAs (100) substrates. A magnetic field of 1 T was applied along the easy direction of the in-plane magnetization at $T=100$ K, which was sufficient to saturate the magnetic moment in the sample. In order to protect the surfaces from oxidation, the films were capped with 20 and 40 Å of aluminum. In the 20 Å aluminum capped films, multiplet features were observed in the XAS spectra due to oxidation of the surface. However, 40 Å aluminum capping was sufficient to protect the film surface since no additional features were observed in that case. Figures 2 and 3 show details of the Co and Mn $L_{2,3}$ XMCD and XAS spectra for the Co_2MnSn film.

Figure 2(a) shows the polarization dependent x-ray absorption spectra (XAS) at the Co $L_{2,3}$ edges of the Co_2MnSn film. There are two XAS spectra shown: XAS_+ is for the parallel relative orientation of the magnetization and x-ray (circular) polarization, whereas XAS_- is for antiparallel orientation. These spectra were taken while keeping the magnetization direction fixed and switching the polarization of the incoming light. The angle of incidence of the (>96%) polarized light was 45°, and the data have been corrected for incident angle and incomplete polarization. The background subtraction was formulated as a step function that matched the pre-L_3 and post-L_2 baselines. The intermediate step between the L_3 and L_2 lines was set at 2/3 the difference between the pre-L_3 and post-L_2 baseline intensities, consistent with its $2j+1$ quantum degeneracy. The linearly polarized XAS (which is the average of XAS_+ and XAS_-) after removing the background, and the integral over the (L_3+L_2) (denoted by r in the figure) are shown in Fig. 2(b). The XMCD (which is the difference between XAS_+ and XAS_-) and the integrals of the XMCD over L_3 (p) and L_3+L_2 (q) are shown in Fig. 2(c).

The sum rules, as given by Chen *et al.*,[21] expressed in terms of p, q, r, and n_d, are $m_{\text{orbital}}=-4q(10-n_d)/3r$ and $m_{\text{spin}}=-(6p-4q)(10-n_d)/r$ in units of Bohr magnetons per atom. The parameter n_d is the 3_d electron occupation number (i.e., or the term $10-n_d$ is the number of d-electron holes) for the transition metal atom in question (Co or Mn in this case).[21] The 3_d electron occupation number can be determined experimentally through absolute white line measurements (usually done by measuring XAS in transmission mode) or from electronic structure calculations. The ratio of the two moments is given by $m_{\text{orbital}}/m_{\text{spin}}=2q/(9p-6q)$, which is independent of both r and n_d.

Figure 3 shows a similar display of spectra for the Mn $L_{2,3}$ edge. Table I summarizes the results obtained for the Co_2MnSn film from the sum rules expressed above without correcting for saturation effects, along with the previously

TABLE I. The magnetic moment components as determined from XMCD spectra for the Co_2MnSn film. The spin, orbital, and total magnetic moments are given by m_S, m_L, and m_T, respectively. The (a), (b), and (c) denote the previously reported values in Refs. 22–24.

Atom	m_S (μ_B)	m_L (μ_B)	m_T (μ_B)	m_L/m_S	n_d (electrons per atom)	Total moment per formulaunit (μ_B)		
Mn	3.52 3.12(7)[a]	0.12 0.09(3)[a]	3.64 3.21[a] 3.58[b]	0.035 0.029[a]	6.71[a]	Our result	Ref. 23	Ref. 22
Co	0.76 0.7[c] 0.85(6)[a]	0.085 0.1[c] 0.02(5)[a]	0.84 0.8[c] 0.87[a] 0.75[b]	0.11 0.14[c] 0.024[a]	9.13[a]	5.32	5.12[d] 4.78[e]	5.08(5)

[a]Reference 23.
[b]Reference 22.
[c]Reference 24.
[d]Magnetic moment from neutron diffraction measurements.
[e]Magnetic moment from saturation magnetization measurements.

reported (calculated and experimental) values.[22–24] Notably, the reported values in Refs. 22 and 23 have large error bars. The values of n_d were taken from the theoretically calculated values by Brown *et al.*[23] The total magnetic moment per formula unit from this calculation is $5.32\mu_B$, which is higher than the obtained bulk value of $4.94\mu_B$. It is natural to expect a slightly higher value compared to the bulk because we have not accounted for the contribution from Sn which is likely antiferromagnetically aligned to the Co and Mn moments, but this alone cannot account for the higher value of moment. However, the Co moments are very close to the theoretical calculations by Ishida *et al.*[24] They have predicted from electronic structure calculations that, in Co_2YZ-type Heusler alloys, the Co atom contains a significantly large orbital moment (which is not quenched, unlike other elements in place of Co), which is consistent with our experimental result. The largest contribution to the total magnetic moment comes from the Mn atoms. Therefore, the larger value of total magnetic moment may have come from the excess manganese concentration, which was seen from compositional analysis of the films using RBS measurements, but this has not been confirmed. In fact, the role of excess Mn depends on the sites in which the excess atoms reside and could actually antialign with the sublattice. Additionally, there are inherent errors in the sum rules, e.g., we have neglected the dipole term $\langle T_Z \rangle$ and also the experimental error which could occur in sample orientation, degree of polarization, self-absorption, and saturation effects. Saturation effects lead to a smaller r, and therefore a larger moment, which could be another reason for the larger moment. The value of n_d was taken from theoretical calculations which can vary greatly depending on the method used to estimate it. Moreover, the overlap of the L_3 and L_2 edges in Mn XMCD spectrum also affects the sum rules results.

Since there are no reported values of the $3d$ occupation number (n_d) for Co_2MnSb, we have not reported the individual moments but rather the ratios of the orbital to spin moments for the Mn and Co atoms which were found to be 0.021 and 0.121, respectively. The corresponding values for Co_2MnSn are 0.035 (Mn) and 0.110 (Co) which, in the case of Co, is large but slightly lower than the predicted value of 0.14.[24]

The XMCD spectra for Co_2MnSn and Co_2MnSb at the Co and Mn $L_{2,3}$ edges are shown in Fig. 4. For a relative comparison, the XMCD data have been normalized to the maximum XAS intensity, where the XAS pre- and postedges have been normalized to zero and one, respectively. The data in Fig. 4 were then expressed as a percent change (relative to the corresponding maximum normalized L_3 XAS intensity) in order to make a qualitative relative comparison. Co_2MnSb is predicted to have a larger magnetic moment per formula unit than Co_2MnSn by the Slater–Pauling curve, where the predicted values are $6\mu_B$ and $5\mu_B$, respectively.[25] However, bulk measurements fall short of these values: $4.94\mu_B$ in Co_2MnSn and, more severely, $5.09\mu_B$ in Co_2MnSb.[26] The XMCD of Co_2MnSb is enhanced relative to that of Co_2MnSn (and more pronounced in the Mn XMCD), which may imply an overall larger moment in the Sb alloy. However, n_d for Co_2MnSb needs to be known for a more complete understanding.

A relative shift of about 0.25 eV was observed in the Mn and Co XMCD spectra of Co_2MnSb and Co_2MnSn (Fig. 4). Although no definitive conclusions can be drawn regarding the origin of the shift, it could be due to an energy shift of the monochromator between scans. However, a shift should also be expected due to the electronic structure differences between the two alloy systems, i.e., Fermi energy shifts and changes in core level binding energies.

CONCLUSIONS

In conclusion, polycrystalline targets were fabricated and were used to deposit magnetic thin films of Co_2MnSn and Co_2MnSb on GaAs (100) using pulsed laser deposition. The element specific magnetic properties of the films were studied using XMCD techniques, and their structural and compositional characteristics were determined. The films were highly crystalline, *sp*-element deficient, and Mn rich. This noncongruent transfer from target to film may be corrected

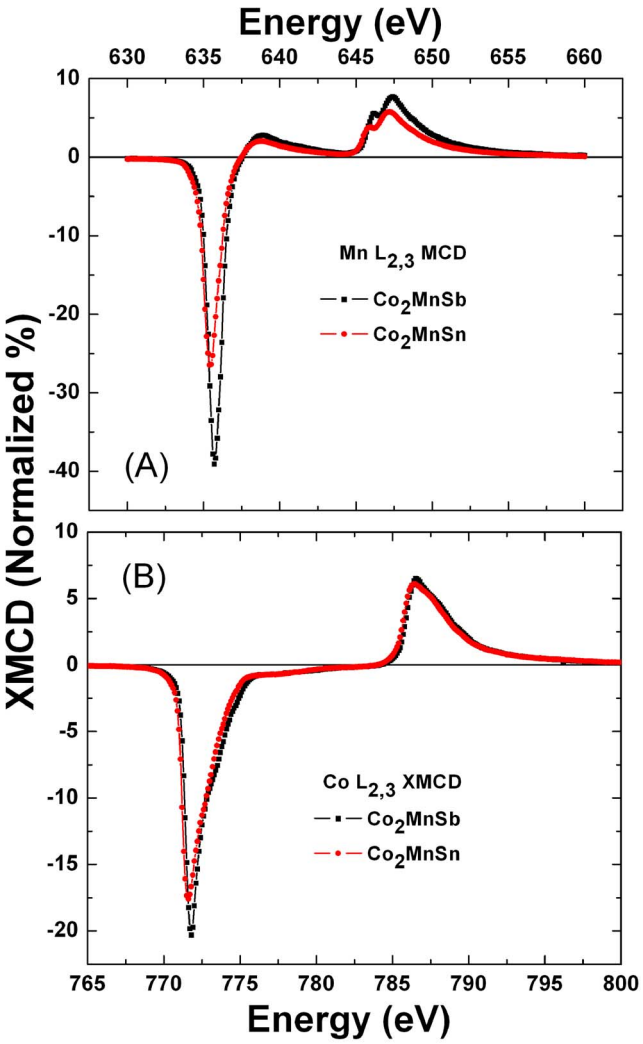

FIG. 4. (Color online) Comparative XMCD intensities of the Co_2MnSn and Co_2MnSb thin films expressed as a percent change relative to the maximum L_3 XAS spectrum for (a) the Mn $L_{2,3}$ edges and (b) the Co $L_{2,3}$ edges.

by using single crystal targets. In the case of the Co_2MnSn film, XMCD was used to estimate the total magnetic moment per formula unit ($5.32\mu_B$), which was found to reside in the range of previously reported values and close to the Slater–Pauling value. The orbital to spin moment ratio was determined for both alloys, and the value for that of Co in Co_2MnSn (0.11) was reasonably close to the theoretical value (0.14). The corresponding value for Co_2MnSb had a larger orbit-spin moment ratio (0.121), and an enhanced XMCD intensity that was more pronounced for the Mn atom, implying that Co_2MnSb film had a larger moment per formula unit, consistent with theoretical predictions.

ACKNOWLEDGMENTS

This work is supported by NSF Grant No. NSF-DMR-0545728. The Advanced Photon Source is supported by the U.S. Department of Energy, Office of Science, under Contract No. DE-AC02-06CH11357.

[1] J. M. Kikkawa and D. D. Awschalom, Nature (London) **397**, 139 (1999).
[2] W. A. Picket and J. S. Moodera, Phys. Today **54**(5), 39 (2001).
[3] G. A. Prinz, Science **282**, 1660 (1999); G. A. Prinz, Phys. Today **48**(4), 58 (1995).
[4] R. A. de Groot, F. M. Mueller, P. G. van Engen, and K. H. J. Buschow, Phys. Rev. Lett. **50**, 2024 (1983).
[5] I. Galanakis, P. H. Dederichs, and N. Papanikolaou, Phys. Rev. B **66**, 134428 (2002).
[6] M. Zhang, Z. Liu, H. Hu, G. Liu, Y. Cui, G. Wu, E. Bruck, F. R. de Boer, and Y. Li, J. Appl. Phys. **95**, 7219 (2004).
[7] S. Ishida, S. Fuji, S. Kashiwagi, and S. Asano, J. Phys. Soc. Jpn. **64**, 2152 (1995).
[8] I. Galanakis, P. H. Dederichs, and N. Papanikolaou, Phys. Rev. B **66**, 174429 (2002).
[9] R. J. Soulen, Jr., J. M. Byers, M. S. Osofsky, B. Nadgorny, T. Ambrose, S. F. Cheng, P. R. Broussard, C. T. Tanaka, J. Nowak, J. S. Moodera, A. Barry, and J. M. D. Coey, Science **282**, 85 (1998).
[10] J.-H. Park, E. Vescovo, H.-J. Kim, C. Kwon, R. Ramesh, and T. Venkatesan, Nature (London) **392**, 794 (1998).
[11] J.-H. Park, E. Vescovo, H.-J. Kim, C. Kwon, R. Ramesh, and T. Venkatesan, Phys. Rev. Lett. **81**, 1953 (1998).
[12] H. Kato, T. Okuda, Y. Okimoto, Y. Tomioka, K. Oikawa, T. Kamiyama, and Y. Tokura, Phys. Rev. B **69**, 184412 (2004).
[13] I. Galanakis, Phys. Rev. B **66**, 012406 (2002).
[14] T. Shishidou, A. J. Freeman, and R. Asahi, Phys. Rev. B **64**, 180401 (2001).
[15] I. Galanakis and P. Mavropoulos, Phys. Rev. B **67**, 104417 (2003).
[16] A. Stroppa, S. Picozzi, A. Continenza, and A. J. Freeman, Phys. Rev. B **68**, 155203 (2003).
[17] H. Akai, Phys. Rev. Lett. **81**, 3002 (1998).
[18] J. J. Kavich, M. P. Warusawithana, J. W. Freeland, P. Ryan, X. Zhai, R. H. Kodama, and J. N. Eckstein, Phys. Rev. B **76**, 014410 (2007).
[19] T. Ambrose, J. J. Krebs, and G. A. Prinz, Appl. Phys. Lett. **76**, 22 (2000).
[20] W. Kraus and G. Nolze, J. Appl. Crystallogr. **29**, 301 (1996).
[21] C. T. Chen, Y. U. Idzerda, H.-J. Lin, N. V. Smith, G. Meigs, E. Chaban, G. H. Ho, E. Pellegrin, and F. Sette, Phys. Rev. Lett. **75**, 152 (1995).
[22] P. J. Webster, J. Phys. Chem. Solids **32**, 1221 (1971).
[23] P. J. Brown, K. U. Neumann, P. J. Webster, and K. R. A. Ziebeck, J. Phys.: Condens. Matter **12**, 1827 (2000).
[24] S. Ishida, Y. Otsukay, Y. Kubo, and J. Ishida, J. Phys. F: Met. Phys. **13**, 1173 (1983).
[25] I. Galankis and P. Mavropoulos, J. Phys.: Condens. Matter **19**, 315213 (2007).
[26] M. R. Paudel, C. S. Wolfe, H. Patton, I. Dubenko, N. Ali, J. A. Christodoulides, and S. Stadler, J. Appl. Phys. **105**, 013716 (2009).